Potential overestimation of community respiration in the western Pacific boundary ocean: what causes the putative net heterotrophy in oligotrophic systems?

Yibin Huang[1,2], Bingzhang Chen[3], Bangqin Huang[1,2*], Hui Zhou[4,5,6], Yongquan Yuan[5,7,8]

[1]State Key Laboratory of Marine Environmental Science, Xiamen University, Xiamen, China

[2]Fujian Provincial Key Laboratory of Coastal Ecology and Environmental Studies, Xiamen University, Xiamen, China

[3]Department of Mathematics and Statistics, University of Strathclyde, Glasgow, United Kingdom

[4]Key Laboratory of Ocean Circulation and Waves, Institute of Oceanology, Chinese Academy of Sciences, and Function Laboratory for Ocean Dynamics and Climate, Qingdao National Laboratory for Marine Science and Technology, Qingdao, China

[5]Center for Ocean Mega-Science, Chinese Academy of Sciences, Qingdao, China

[6]University of Chinese Academy of Sciences, Beijing, China

[7]Key Laboratory of Marine Ecology and Environmental Sciences, Institute of Oceanology, Chinese Academy of Sciences, Qingdao, China

[8]Laboratory for Marine Ecology and Environmental Science, Qingdao National Laboratory for Marine Science and Technology, Qingdao, China

Running head: Plankton respiration in western Pacific

Keywords: Gross primary production; Community respiration; Net community production; Bacterial production; Western Pacific Ocean; Metabolic state

Email address: Yibin Huang (ybhuang@stu.xmu.edu.cn); Bingzhang Chen (bingzhang.chen@strath.ac.uk); Bangqin Huang (bqhuang@xmu.edu.cn); Hui Zhou (zhouhui@qdio.ac.cn); Yongquan Yuan (zyu@qdio.ac.cn);

*** Correspondence:** Bangqin Huang (bqhuang@xmu.edu.cn)

Abstract

Microbial metabolism is of great importance in affecting the efficiency of biological pump and global carbon cycles. However, the metabolic state of the oligotrophic ocean, the largest biome on Earth, remains contentious. We examined the planktonic and bacterial metabolism using *in vitro* incubations along the western Pacific boundary during September and October 2016. The integrated gross primary production (GPP) of the photic zone exhibited higher values in the region of 2°-8°N along 130°E and the western Luzon Strait, which is consistent with the regional variability of nutrients in the different ocean provinces. Spatially, the community respiration (CR) was less variable than the GPP and slightly exceeded the GPP at most of the sampling stations. Overall, the *in vitro* incubation results suggest a prevailing heterotrophic state in this region. A comparison of the metabolic rates from the *in vitro* incubations with recently published biogeochemical model results in the same region shows that our observed GPP values were close to those predicted by the model, but the measured CR was approximately 30% higher than the modelled values. We also found that most of the *in vitro* CR estimates were higher than the upper range of the empirical CR estimated from the sum of the contributions of the main trophic groups. Conversely, the estimates of the empirical CR support the rationality of the CR predicted by the biogeochemical model. In general, the results indicate that systematic net heterotrophy is more likely a result of the

47 overestimation of CR measured by the light-dark bottle incubation experiments, although
48 the exact cause of the methodological problem remains unknown.
49

Introduction

Biological carbon production and consumption are two important ecological processes in the marine system and contribute significantly to the global carbon cycles [*Longhurst*, 1995]. Marine phytoplankton are responsible for almost half of global primary production [*Field et al.*, 1998]. Most of the organic carbon produced via photosynthesis is remineralized by heterotrophic organisms and released as dissolved inorganic carbon, and a tiny fraction of the particulate organic carbon is exported into the deep ocean, which is the so-called *biological pump* process [*Sigman and Boyle*, 2000]. The difference between the gross primary production (GPP) and community respiration (CR), termed net community production (NCP), should theoretically be equal to the amount of organic carbon available for potential export and thus is suggested to be one of the best descriptors of the role of biota in oceanic absorption or release of atmospheric CO_2 [*Ducklow and Doney*, 2013; *Giorgio et al.*, 2005]. Increasing amounts of evidence indicate that in addition to primary production, the variability and magnitude of heterotrophic respiration also play important roles in the emergence of the geographic patterns of NCP or export production [*Aranguren-Gassis et al.*, 2011; *Serret et al.*, 2015]. Therefore, accurate assessments of autotrophic and heterotrophic metabolism are required for a more comprehensive understanding of the efficiency of the biological pump at the global scale.

69 Over the last several decades, the metabolic state in the oligotrophic ocean has been
70 actively debated in oceanography; the NCP signals derived from the *in vitro* incubation
71 approach, typically using light-dark bottles, suggest a prevalence of heterotrophy in the
72 oligotrophic ocean, which is in sharp contrast with the consistently positive NCP signals
73 derived from incubation-free methods [*C. M. Duarte et al.*, 2013; *Ducklow and Doney*,
74 2013; *P J L Williams et al.*, 2013]. The advantage of the incubation approach is that it
75 allows us to estimate the integrated NCP from discrete depths and over 24 h, whereas
76 most incubation-free techniques can only constrain the integrated rates at fixed depths,
77 typically within the surface mixed layer. *C. M. Duarte et al.* [2013] compiled a global
78 incubation-based dataset, and the scaling functions suggest that the open ocean, with
79 values of GPP and chlorophyll-*a* (Chl-*a*) concentrations less than 2 mmol O_2 m^{-3} d^{-1} and
80 0.44 mg m^{-3}, respectively, tend to be systematically heterotrophic. In addition, *Regaudie-*
81 *de-Gioux and Duarte* [2012] examined the sensitivity of primary production and
82 respiration to temperature, and the results implied higher activation energy of respiration
83 (0.66 ± 0.05 eV) than primary production (0.32 ± 0.04 eV). The implication is that all
84 other things being equal, the CR is likely to exceed the GPP in the tropical and
85 subtropical ocean. However, the purported heterotrophy suggested by in vitro incubation
86 remains questionable in part because the carbon deficit is difficult to sustain based on the
87 current understanding of ocean carbon cycling [*Ducklow and Doney*, 2013; *P J L*
88 *Williams et al.*, 2013]. Recent improvements in understanding this controversy were

89 attempted by *Letscher and Moore* [2017], who first included globally optimized
90 dissolved organic carbon cycling into an ecosystem-circulation ocean model to assess the
91 metabolic rates around the global ocean, which provides a powerful approach to validate
92 the observations of the metabolic state from a geochemical perspective.

93 Bacteria play a vital role in the nutrient and organic cycle [*Arrigo*, 2005] and mediate
94 the carbon transfer efficiency from lower to higher trophic levels through the microbial
95 loop, which in turn influences the organic export [*Azam et al.*, 1983; *Jiao et al.*, 2010].
96 Bacterial respiration has been commonly considered to be the major part of CR.
97 Especially in some unproductive marine ecosystems, bacterial respiration has been
98 suggested to even exceed the net primary production [*Del Giorgio et al.*, 1997].
99 However, this view was challenged by *Calbet and Landry* [2004], who argued that
100 because microzooplankton consume a substantial proportion (-70%) of primary
101 production, their contribution to CR must not be negligible. Thus, quantification of
102 bacterial activity is critical for defining the metabolic balance.

103 The western Pacific Ocean is a particularly important region in regulating the global
104 ocean circulation and climate system by the active exchange and transport of water, heat
105 and salinity with adjacent tropical and subtropical oceans [*Hu et al.*, 2015]. The currents
106 in the epipelagic zone are complicated and mainly include the North Equatorial Current
107 (NEC), North Equatorial Countercurrent (NECC), Subtropical Countercurrent (STCC),

Kuroshio Current (KC) and Mindanao Current (MC) [*Hu et al.*, 2015]. This area is a water-mass crossroads [*Fine*, 1994] and is also a typical tropical-subtropical oligotrophic environment that is characterized by very low Chl-*a* and nutrient concentrations in the upper ocean [*G Yang et al.*, 2017c]. The present knowledge about this region is particularly focused on the hydrographic dynamics (see the review of *Hu et al.* [2015]), and the biological processes have been explored much less except for several reports on the geographic patterns of zooplankton distributions [*G Yang et al.*, 2017b] and nitrogen fixation [*Shiozaki et al.*, 2009]. The aim of this study is to determine the geographic pattern of planktonic and bacterial activity in the region of the still undersampled western Pacific boundary. Although incubation experiments using light-dark bottles are a straightforward and widely used method to measure metabolic rates in various environments, the different results in the oligotrophic ocean between this method and other incubation-free methods suggest that there might be a bias with this method, particularly in oligotrophic warm oceans [*C. M. Duarte et al.*, 2013; *P J L Williams et al.*, 2013]. Of course, each methodology has its own assumptions and potential limitations. It is desirable to compare methods to reduce the uncertainty and enhance our understanding of the metabolic state of the oligotrophic ocean, which is the largest biome on Earth. Specifically, we compare our observational results with those of an excellent modelling study of the metabolism of the global ocean [*Letscher and Moore*, 2017]. We also try to

estimate CR by summing the contributions of major trophic groups based on independent measurements and various conversion factors reported in the literature.

Based on these arguments, we ask the following two sets of questions:

1. Can we observe the net heterotrophic state in the tropical-subtropical and oligotrophic western Pacific boundary using the *in vitro* incubation method following the scaling laws proposed by Duarte et al. (2013)? Will the results be consistent with the model results of Letscher and Moore (2017) and other estimates? If the answers are yes, then we should search for evidence of lateral transport of dissolved organic matter in this region.

2. If the estimated NCP rates differ between methodologies, what are the sources in terms of the GPP or CR that cause this discrepancy? In other words, what types of measurements are the most likely to be biased?

Methods

Study sites

The cruise was conducted in the western North Pacific Ocean along two transects at 130°E (2°N- 20°N) and 20°N (120°E-132°E) from 7 September to 9 October, 2016, on RV *"KEXUE"* (Fig. 1). A total of 31 stations were investigated, and 11 stations were used for incubation experiments (red triangles in Fig. 1). The approximate fields of the main currents in the western North Pacific are shown in Fig. 1.

146

147 **Physical and chemical measurements**

148 The water temperature and salinity at each station were measured using a Sea-Bird
149 Electronics CTD SBE 911plus probe. The CTD probe was calibrated immediately before
150 the cruise. To determine the concentrations of inorganic nitrate plus nitrite, ammonium
151 and silicate and phosphate, 100 ml water samples were collected at 6-8 discrete depths
152 from 0 to 300 m using 20 L Niskin metal-free bottles attached to the rosette of the CTD.
153 The water samples were subsequently analyzed using a Skalar Flow Analyzer (Skalar
154 Ltd., Netherland), and the data quality was estimated via inter-calibration. The depth of
155 the nitracline was determined as the depth where the nitrate concentration reached 5
156 mmol m^{-3}. The nitrate gradient across the base of the euphotic zone at each station was
157 calculated as an index of the potential availability of nutrients in the euphotic zone by
158 vertical diffusion from the deeper layer.

159

160 **Biological measurements and *in vitro* oxygen-based metabolism**

161 Seawater samples from five discrete depths, corresponding to 100%, 50%, 10%, and
162 1% of the surface incident irradiance and the deep chlorophyll maximum (DCM), were
163 collected at the incubation stations above 200 m water depth before dawn. If the depth of
164 the DCM was coincident with the depth of 10% or 1% surface incident irradiance, an

165 additional depth between the layers of 50% and 1% surface incident irradiances was
166 sampled. The sampled water was transferred into 10 L acid-cleaned carboys using a
167 silicone tube. One L of water was filtered onto a Whatman GF/F filter to measure the Ch-
168 *a* concentration. The Ch-*a* was extracted using 90% aqueous acetone in dark conditions
169 for 12-20 h at 4°C and then measured by a Turner Trilogy fluorometer [*Welschmeyer*,
170 1994].

171 The planktonic community metabolic rates were estimated from the changes in
172 dissolved oxygen concentrations in the light-dark bottles over a 24-hour incubation
173 period following the procedure of *Serret et al.* [1999]. The dissolved oxygen
174 concentrations were determined by high-precision Winkler titration [*Huang et al.*, 2018;
175 *Oudot et al.*, 1988] with an automated potentiometric end-point detection system
176 (Metrohm-848, Switzerland). For each depth, the water samples were carefully siphoned
177 into twelve calibrated 100 ml borosilicate bottles using silicon tubing, with more than 300
178 ml overflowing. Then, four replicate bottles were immediately fixed by the Winkler
179 regents with $MnCl_2$ (3 mol L^{-1}) and NaI (4 mol L^{-1})/NaOH (8 mol L^{-1}) to quantify the
180 initial dissolved oxygen concentrations. The four light bottles were covered by neutral
181 density meshes to adjust the light conditions to *mimic the in situ* irradiances of the
182 corresponding sampling depths. The remaining quadruplicate bottles were placed inside
183 dark bags as dark bottles. Both the light and dark bottles were incubated in a large tank

184 on the deck filled with running seawater pumped from the surface ocean and exposed to
185 natural sunlight. After the 24-hour incubation period, the dissolved oxygen
186 concentrations in the bottles were determined. GPP was calculated as the difference
187 between the average dissolved oxygen concentrations in the light and dark bottles, and
188 CR was calculated as the difference between the average dissolved oxygen
189 concentrations in the initial and dark bottles. NCP was equal to GPP-CR. The average
190 percentage coefficients of variation (% ratio of the standard deviation to the mean) of the
191 dissolved oxygen replicates were 0.15%, 0.17% and 0.17% for the initial, light and dark
192 bottles, respectively. The complete data set will be deposited in the public global
193 respiration database: https://www.uea.ac.uk/environmental-sciences/people/profile/carol-
194 robinson#researchTab (the dataset is maintained by Carol Robinson).

195 We noted that the on-deck incubation is subject to some problems such as changes of
196 *in situ* light and temperature condition for the submarine samples during the incubation.
197 The metabolic rates are temperature-dependent [*López-Urrutia et al.*, 2006; *Regaudie-de-*
198 *Gioux and Duarte*, 2012]. The temperature in the incubator maintained by the running
199 surface seawater would artificially elevate the *in situ* temperature conditions for the
200 subsurface samples during the incubation. To minimize this effect, the metabolic rates
201 below the surface were corrected by the activation energy of the GPP and CR reported by
202 Regaudie-de-Gioux and Duarte 2012 (Supporting Information). It is also well known that

203 the spectral characteristics of submarine light differ from those of surface light, featured
204 with a higher fraction of blue light [*Clarke and Oster*, 1934]. The use of neutral density
205 screen in our study well simulated the attenuation of submarine light intensity, but failed
206 to simulate submarine spectral composition. Since the peak absorption bands of most
207 algal pigments lie in the blue region of the visible light spectrum, the Chl-*a* specific
208 absorption coefficient for the phytoplankton in the sub-surface ocean would be higher in
209 the same intensity dominated by blue light than white light. A previous study of *Edward*
210 *A. Laws et al.* [1990] showed that real primary production rates would be underestimated
211 by a factor of two if incubations are performed using surface light attenuated with neutral
212 density screen. In the present study, the sampling depths were identified as different
213 gradients of broad-band surface light estimated by the depth-averaged attenuation
214 coefficient of water column (K_{mean}). A study by *Kyewalyanga et al.* [1992] suggested that
215 water-column primary production integrated from the sampling depths determined by
216 K_{mean} was not significantly different from the real primary production. Their results
217 indicated that light filed judged by K_{mean} gave higher light intensity at all depths
218 compared to light intensity calculated using the spectral light value, then resulting in
219 overestimating the *in situ* primary production. Thus, the negative bias due to the
220 difference of spectral characteristics in the submarine would be partly compensated by
221 the positive bias inherited from overestimated light intensity, leading to a final integrated
222 value of primary production close to the real primary production. In the future study,

223 more improvements are expected to accurately achieve ambient *in situ* light condition and
224 reduce the uncertainty by using the neutral and blue density screening or the incubation
225 buoy if possible.

226

227 **Bacterial production**

228 Bacterial production (BP) was measured followed the protocols of ^{3}H-lecine
229 incorporation [*Chen et al.*, 2014; *Kirchman*, 1993]. Four 1.8-mL aliquots of water were
230 collected from each depth and added to 2-mL sterile microcentrifuge tubes (Axygen, Inc.,
231 USA), and they were incubated with a saturating concentration (10 nmol L^{-1}) of ^{3}H-
232 lecine (Perkin Elmer, USA) for 2 hours in the dark. One sample was immediately killed
233 by adding 100% trichloroacetic acid (TCA) as a control, and the other three incubations
234 were stopped by the addition of TCA at the end of the 2-hour incubation. Five vacuum
235 cups filled with the seawater from the corresponding sampling depths were used as the
236 incubators for BP to stimulate the *in situ* temperature during the 2-hour incubation. After
237 the incubation, the water samples were filtered onto 0.2-μm polycarbonate filters (GE
238 Water & Process Technologies, USA). The filters were rinsed twice with 3 mL of 5%
239 TCA and twice with 2 mL of 80% ethanol before being frozen at -20°C. Upon return to
240 the laboratory, the dried filters were placed in scintillation vials with 5 mL of Ultima
241 Gold scintillation cocktail (Perkin-Elmer, USA). The radioactivity retained on the filters

242 was measured as disintegrations per minute using a Tri-Carb 2800TR liquid scintillation
243 counter (Perkin Elmer, USA). The rate of incorporation of ^{3}H leucine was calculated
244 from the difference between the treatment and control tubes.

245 Seven experiments were conducted to determine empirical factors to convert from
246 the leucine incorporation rates to bacterial carbon production. Predator-free water was
247 obtained by filtering seawater through 1 μm polycarbonate membrane filters and then
248 diluted to 10% by 0.2 μm filtered seawater. The leucine incorporation rates and bacterial
249 abundance were monitored every 4 to 6 hours for a maximum of 2 days. The cumulative
250 method was used to derive the empirical conversion factor by linear regression of the
251 bacterial number yields against the integrated leucine incorporation rates [*Bjørnsen and*
252 *Kuparinen*, 1991]. The factor of 30.2 fg C cell^{-1} was applied to convert bacterial
253 abundance to carbon biomass [*Fukuda et al.*, 1998]. The conversion factors in our
254 measurements varied from 0.20 to 0.91 kg C mol Leu^{-1}, and we used the geometric mean
255 value of 0.37 kg C mol Leu^{-1} to convert the incorporation of leucine to carbon units.

256

257 **Integrated metabolism rates derived from the biogeochemical ocean model**

258 The model-based metabolism used in our study was based on the results derived
259 from a recently published biogeochemical model in the same region [*Letscher and*
260 *Moore*, 2017]. We chose this model because the organic carbon concentrations are well

calibrated in the model. In *Letscher and Moore* [2017], three types of allochthonous organic carbon sources (contemporary rivers, atmospheric deposition and realistic semi-labile and refractory marine dissolved organic carbon pool) were integrated into the Biogeochemical Elemental Cycling (BEC) v1.2.2 module of the Community Earth System Model (CESM). The model outputs include both GPP and CR within the euphotic zone, which allows us to directly compare them with our measured values from the light-dark bottles. In addition, the physical forcing of the western Pacific boundary has been well resolved in the ecosystem-circulation model; therefore, we feel confident that the results in this region would be reasonable.

Briefly, the GPP in this model was computed from the phytoplankton nitrogen demand satisfied by nitrate, ammonium, and N_2-fixation. CR was calculated as the sum of the carbon losses induced by the mortality of phytoplankton and zooplankton, phytoplankton grazed by zooplankton, and respiration of both particulate and dissolved organic carbon. Therefore, NCP is equal to GPP minus CR. The horizontal resolution of the model outputs is $1° \times 1°$ with a higher resolution near the equator. The vertical resolution is 10 m in the upper 160 m. The daily volumetric metabolism (GPP and CR) from the model output is monthly climatology with 20-year averages (1946-2007) in units of mmol O_2 m^{-3} d^{-1}. The integrated euphotic GPP and CR were calculated by trapezoidal integration of the volumetric data from the surface to the depth of 1% incident

280 irradiance (typically 100-120 m in this study). Because our study was conducted between
281 September and October, we compared our results with the model outputs for both
282 September and October. The spatial variations of the euphotic zone integrated GPP and
283 CR in this region are presented in Fig. S2. To conduct a paired comparison of the
284 metabolism at each sampling station, we extracted the volumetric GPP and CR from the
285 biogeochemical model in the corresponding grid cells within which our sampling stations
286 were located.

287

288 **Estimates of the empirical CR from the contributions of different plankton groups**

289 Because our measured GPP values are consistent with the model results from
290 *Letscher and Moore* [2017] (see Results), we are confident in the GPP estimations in this
291 area and attempt to estimate the respiration rates of major groups based on the GPPs and
292 published growth efficiencies of corresponding groups to provide additional constraints
293 on the CR [*Morán et al.*, 2007; *Robinson et al.*, 2002; *Robinson and Williams*, 2005].
294 Mesozooplankton are usually considered to be poorly sampled by *in vitro* procedures in
295 small volumes (i.e., 100 ml in this study) because of their low abundances. Therefore, we
296 assume that the major groups in our incubation system are composed of heterotrophic
297 bacteria, phytoplankton (dominated by *Prochlorococcus* and *Synechococcus*) and
298 microzooplankton. Considerable errors are associated with the estimates of each group,
299 but importantly, the results showed that even under the conditions of the maximum

300 possible contributions, it is still difficult to bridge the gap between the *in vitro* measured
301 respiration and the estimated respiration.

302 For phytoplankton respiration, *Carvalho et al.* [2017] reported that the global new
303 respiration (which is mainly contributed by phytoplankton) ranges from 10 to 30% of
304 GPP and that the remainder of the respiration (namely, old respiration) is contributed by
305 other groups, including phytoplankton. If phytoplankton account for part of the old
306 respiration as well, the corresponding ratio of phytoplankton respiration to GPP would be
307 similar to the published ratio (-35%) [*Carlos M Duarte and Cebrián*, 1996]. In a lab
308 experiment, *Marra and Barber* [2004] observed that phytoplankton respired up to 40% of
309 daylight primary production when exposed to 12:12 h light:dark conditions. Therefore, it
310 is reasonable to constrain the possible range of phytoplankton respiration assuming a
311 range of 15-40% of daily GPP. Based on a meta-analysis of grazing rates around the
312 global ocean, *Calbet and Landry* [2004] suggested that approximately 50-60% of the
313 GPP in the oligotrophic ocean is grazed by microzooplankton. The growth efficiency for
314 proto- and metazooplankton is generally considered to be in the range of 50-70% based
315 on allometric scaling of protistan growth and respiration rates (Fenchel and Findlay 1983)
316 as well as direct assessments from protistan carbon budgets (e.g., *Verity* [1985]). We also
317 compared three previously reported empirical functions that related the bacterial growth
318 efficiency (BGE) to temperature [*Rivkin and Legendre*, 2001], Chl-*a* [*López-Urrutia and*

319 *Morán*, 2007] and BP [*Roland and Cole*, 1999]. Irrespective of the different assumptions,
320 the resulting values of these three BGEs in our study were strongly correlated and yielded
321 average values of 7.41 ± 0.03% for the temperature-based BGE, 7.93 ± 0.02% for the
322 Chl-*a* based BGE, and 9.09 ± 0.01% for the BP-based BGE (Table S1). These estimated
323 BGEs are very similar to the *in situ* measured BGEs in the offshore stations of the North
324 Atlantic, which have a mean value of 9% [*Alonso-Sáez et al.*, 2007]. Another uncertainty
325 associated with the estimation of the bacterial respiration is CF, which is a crucial
326 parameter for estimating BP and the additional impact on the magnitude of the estimated
327 respiration contributed by bacteria. Our measured CFs varied by a factor of 4.5 (0.2-0.9
328 kg C mol Leu^{-1}) with a mean value of 0.37 kg C mol Leu^{-1}. Admittedly, applying a single
329 mean value of the conversion factor to estimate BP might bias the estimate of bacterial
330 respiration.

331 Based on the studies described above, we attempted to constrain the upper and lower
332 boundaries of the empirical CR at the sampling stations (Table 1). To quantify the upper
333 boundary of the empirical CR, we assumed the case with values of 40% of daily GPP
334 respired by phytoplankton, 60% of daily GPP grazed by zooplankton, 50% zooplankton
335 growth efficiency, 0.9 kg C mol Leu^{-1} of CF and 7.4% of BGE in this region.
336 Correspondingly, we constrained the lower boundary of the empirical CR by assuming
337 that 15% of daily GPP is respired by phytoplankton, 30% of daily GPP is grazed by

zooplankton, the zooplankton growth efficiency is 70%, CF is 0.2 kg C mol Leu^{-1}, and BGE is 9.1% in this region.

Table 1. Estimates of the empirical community respiration contributed by major trophic groups. Details about the calculations are described in the text. Resp: respiration; GPP: gross primary production; BP: bacterial production; BGE: bacterial growth efficiency; CF: conversion factor.

Trophic group	Definition	Methods	References
Phytoplankton	Upper boundary Lower boundary	Resp=0.34*GPP Resp=0.15*GPP	Carvalho et al. (2017) Marra and Barber (2004) Duarte and Cebrián (1996)
Microzooplankton	Upper boundary Lower boundary	Resp=0.65*0.7*GPP Resp=0.5*0.5*GPP	Calbet and Landry (2004) Straile (1997); Fenchel and Findlay (1983); Verity (1985)
Heterotrophic Bacteria	Upper boundary Lower boundary	Resp=(BP/0.07)-BP;(CF=0.90); Resp=(BP/0.09)-BP; (CF=0.2)	López-Urrutia and Morán (2007); Rivkian et al. (2001); Roland and Cole (1999)

Statistical analysis

The rates integrated over the euphotic zone were calculated by trapezoidal integration of the volumetric data from the surface to the depth of 1% incident irradiance. The standard errors for the integrated values were estimated by the propagation procedures for independent measurements described by *Miller and Miller* [1988]. We used a respiratory quotient of 1.2 to convert the carbon-based metabolism to an oxygen basis based on the assumption that inorganic nitrogen was released from organic matter in the form of ammonium [*Hedges et al.*, 2002; *Edward A Laws*, 1991]. All GPP, CR,

NCP and BP values are presented as mean values with standard error. The data were log-transformed to satisfy the assumption of normality, which was confirmed (after transformation) via a Kolmogorov–Smirnov test. The correlations between the variables were examined by Pearson correlation. The linear regressions between the GPP and CR were conducted by reduced major axis regression analysis (model II linear regression) using the R software [*Core*, 2014]. The spatial variabilities of GPP and CR were evaluated by calculating the coefficient of variation (% ratio of the s.d. to the mean) of the integrated metabolism between the stations. The paired *t*-test was conducted to examine the difference between the metabolism rates at each sampling station derived from the O_2-based incubation and the geochemical model predictions. The significance was satisfied if the type I error rate (p) was less than 0.05. Figs. 1 and 2 were plotted using the Ocean Data View software [*Schlitzer*, 2012].

Results

Physical parameters and biochemical characterizations of the two transects

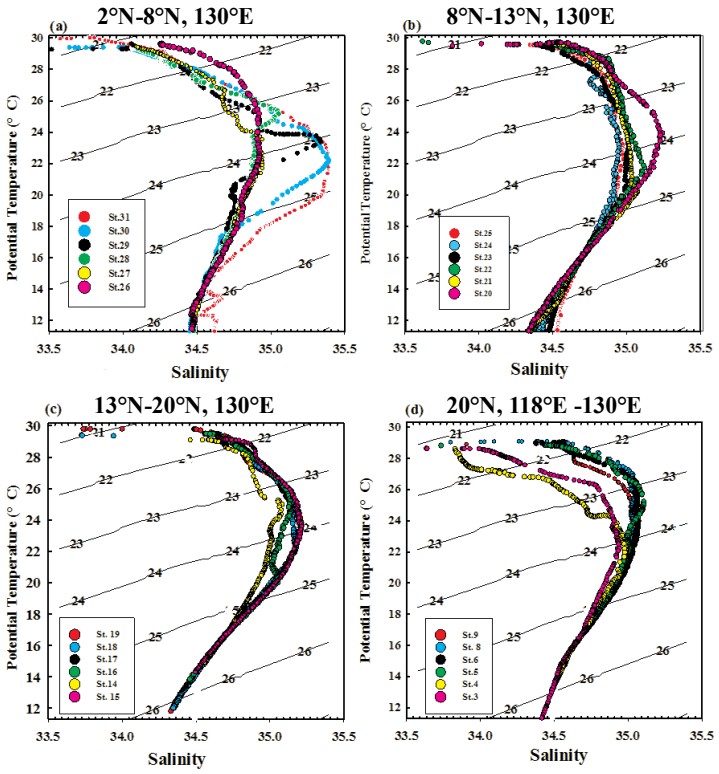

Figure 2. Temperature-salinity diagrams (upper 300 m of water) of the sampling stations in the western Pacific Ocean. Black contours indicate σ_θ (units: potential density-1000 kg m^{-3}). Different colors represent different stations.

The characteristics of the potential temperature and salinity in the upper 300 m for each station are shown in Fig. 2. In this region, the water masses were relatively complicated due to the interactive influences of different currents. In the southernmost stations (St. 29-31), we observed higher salinity (>35.25) at 200-300 m (Fig. 2a). This high salinity water originated from the South Pacific Tropical Water (SPTW) and was carried by the New Guinea Coastal Current (NGCC) and the New Guinea Coastal Undercurrent (NGCUC) from the South Pacific (Qu et al. 1999; Zhou et al. 2010). At St. 17-28, the upper water masses were mainly influenced by the typical NPTW and were characterized by salinities slightly lower (34.75<S<35.25) than the SPTW (Fig. 2b and

382 2c; Fine 1994; Qu et al. 1999). St. 14-16 were located along the boundary between the
383 NEC and the STCC, where energetic meso-scale eddies were very active, and the water
384 masses in this region have both tropical and subtropical gyre characteristics (Fig. 2c). On
385 the transect along 20°N, the water masses at St. 5-9 were dominated by the Kuroshio
386 water, which featured higher salinity and temperature than the water in the adjacent South
387 China Sea (Fig. 2d). At St. 3-4, the upper water was a mixture of relatively fresh and cold
388 water from the South China Sea and saltier and warmer water from the intrusion of the
389 KC at depths of 200-300 m (Fig. 2d).

390 The main hydrographic features along the two transects are shown in Fig. 3. The
391 water along the 130°E transect was characterized by high surface temperatures with a
392 mean value of 29.8 ± 0.2°C. The surface salinity along this transect generally increased
393 from 33.8 at the southernmost station (31) to 34.4 at St. 14. On the transect along 20°N,
394 the temperature and salinity exhibited a westward trend toward colder and less saline
395 waters. The average surface temperature along the 20°N transect (28 .4 ± 0.2°C) was
396 slightly lower than that along the 130°E transect. The lowest salinity along the 20°N
397 transect was observed at the westernmost station (St. 4).

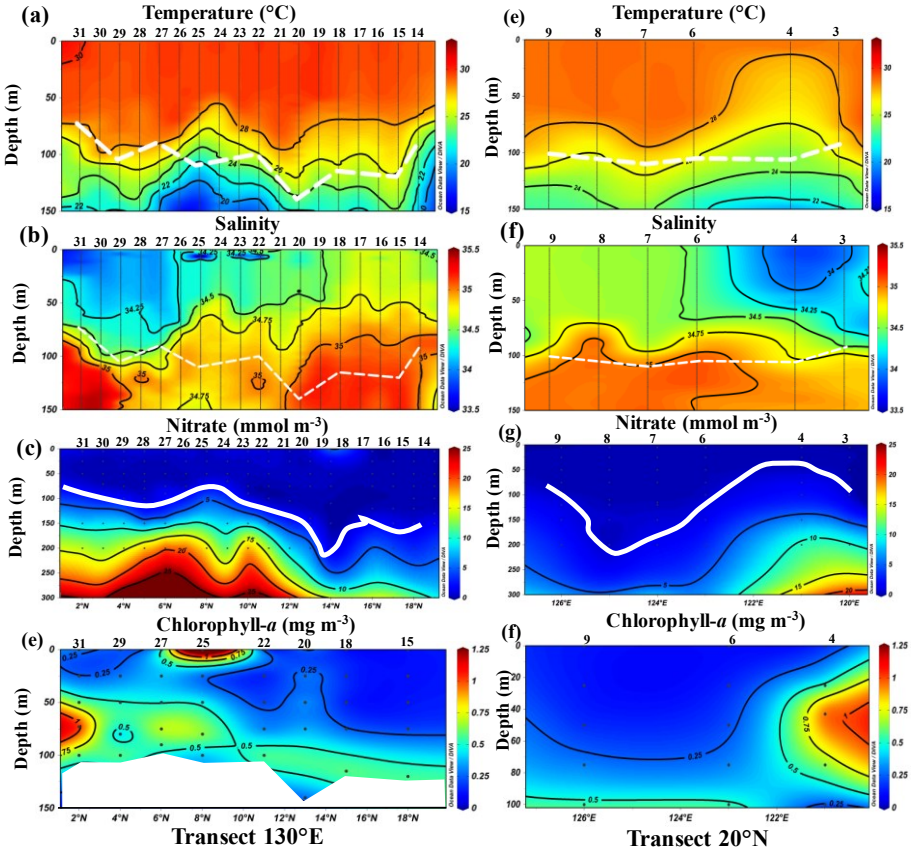

Figure 3. Vertical distributions of temperature, salinity, nitrate and chlorophyll-*a* on the south-north transect along 130°E and the west-east transect along 20°N. The white dashed and white solid lines represent the bottom of the euphotic zone and the depth of the nitracline, respectively. The numbers above the figures indicate the sampling stations.

The depths of the euphotic zone in the two transects (white lines in Fig. 3) were generally at approximately 100-150 m. Along the 130°E transect, the nitrate conditions showed higher concentrations and a shallower depth of the nitracline at 2°-8°N (white dashed lines in Fig. 3e). In the 20°N transect, the lowest average nitrate concentration (0.87 ± 0.37 μmol L^{-1}) in the upper 300 m was found in the region of the eastern Luzon

409 Strait. The patterns of NH_4^+, PO_4^{3-}, and SiO_3^{2-} generally followed the trend of the nitrate
410 concentrations in the water masses (Yu et al., unpublished data).

411 The Chl-*a* concentrations at the incubation stations are shown in Figs. 3e and 3f.
412 Along the 130°E transect, the surface Chl-*a* concentrations were lower in the surface
413 water (<0.25 mg m^{-3}), except for the presence of high values at the surface at St. 27. A
414 well-developed deep Chl-*a* maximum (DCM) was observed at the base of the euphotic
415 zone. The Chl-*a* concentrations at the DCM decreased to the north from 1 mg m^{-3} at St.
416 31 to less than 0.5 mg m^{-3} at St. 15. Along the 20°N transect, shallower DCMs were
417 observed at approximately 50 m in the region of the eastern Luzon Strait compared to the
418 stations to the west.

419

420 **Plankton community metabolism along the two transects**

421 Along the 130°E transect, the volumetric GPP ranged between 0.1 mmol O_2 m^{-3} d^{-1}
422 and 1.2 mmol O_2 m^{-3} d^{-1} and generally decreased with depth (Fig. 4a). Higher volumetric
423 GPPs were found in the region of 2°-8°N (St. 25-St. 31) and were associated with high
424 nitrate and Chl-*a* concentrations. The range of volumetric CRs was similar to that of the
425 volumetric GPP, and the highest volumetric CR was located at the surface at St. 31 (Fig.
426 4b). The vertical gradient of CR was relatively homogenous along this transect (Fig. 4b).
427 The volumetric NCP varied from -0.6 mmol O_2 m^{-3} d^{-1} at the surface at St. 20 to 0.4

mmol O_2 m^{-3} d^{-1} at 70 m at St. 31 (Fig. 4c). Positive volumetric NCPs were mainly located in some surface and subsurface waters at low latitudes (St. 25-31; Fig. 4c). In terms of the euphotic zone integrated metabolism, the integrated GPP generally decreased to the north with higher values in the region of 2°-8°N (Fig. 5a). The spatial variation of the integrated CR had a similar pattern to that of the GPP although with a smaller amplitude (Fig. 5b). The O_2 integrated NCPs at St. 31 and St. 29 were close to zero, whereas a persistent net heterotrophic state was found from 5°N to 20°N (Fig. 5c).

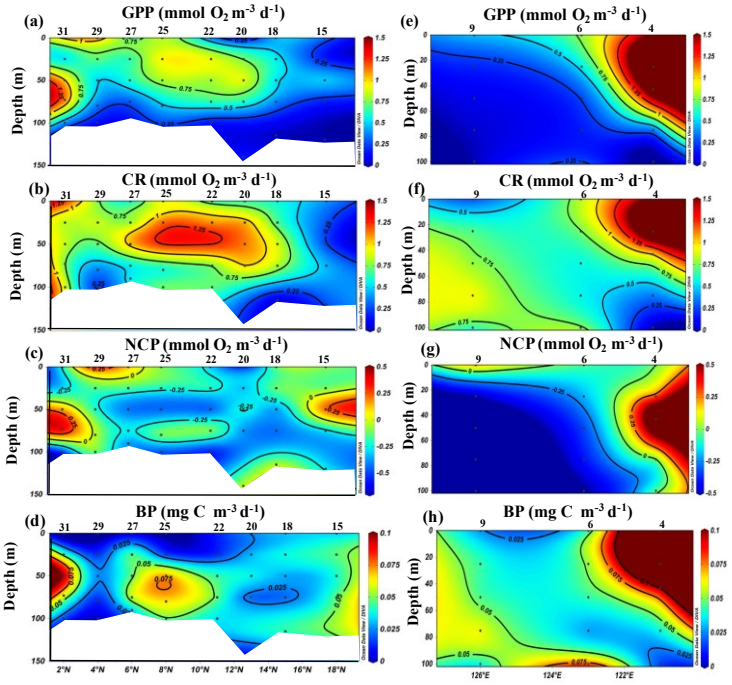

Figure 4. Vertical distributions of volumetric gross primary production (GPP), community respiration (CR), net community production (NCP) and bacterial production (BP) along two transects (130°E and 20°N) in the western Pacific Ocean. The numbers above the figures indicate the sampling stations.

441 For the 20°N transect, the maximum volumetric GPP (2.3 mmol O_2 m^{-3} d^{-1}) was
442 coincident with the occurrence of the maximum volumetric CR (2.1 mmol O_2 m^{-3} d^{-1}) at
443 the surface at St. 4 (Fig. 4e), where the waters were mixed by relatively nutrient-rich
444 seawater from the adjacent South China Sea. At St. 6 and St. 9, which were affected by
445 the oligotrophic KC, the volumetric GPP decreased to very low values, whereas the
446 volumetric CR remained at intermediate values (Fig. 4e and 4f). As a result, positive
447 volumetric NCP was observed throughout the water column at St. 4, and negative NCP
448 was observed at St. 6 and St. 9 (Fig. 4g). The euphotic zone integrated GPP decreased to
449 the east along this transect from 122 mmol O_2 m^{-2} d^{-1} at the westernmost station to 13
450 mmol O_2 m^{-2} d^{-1} at the easternmost station (Fig. 5a). The range of the euphotic zone
451 integrated CR in this transect was only one-third of the GPP, ranging from 66 mmol O_2
452 m^{-2} d^{-1} at St. 9 to 96 mmol O_2 m^{-2} d^{-1} at St. 4 (Fig. 5b). The integrated NCP showed
453 pronounced shifts from a net autotrophic state at St. 4 to heterotrophic at St. 6 and 9 (Fig.
454 5c).
455

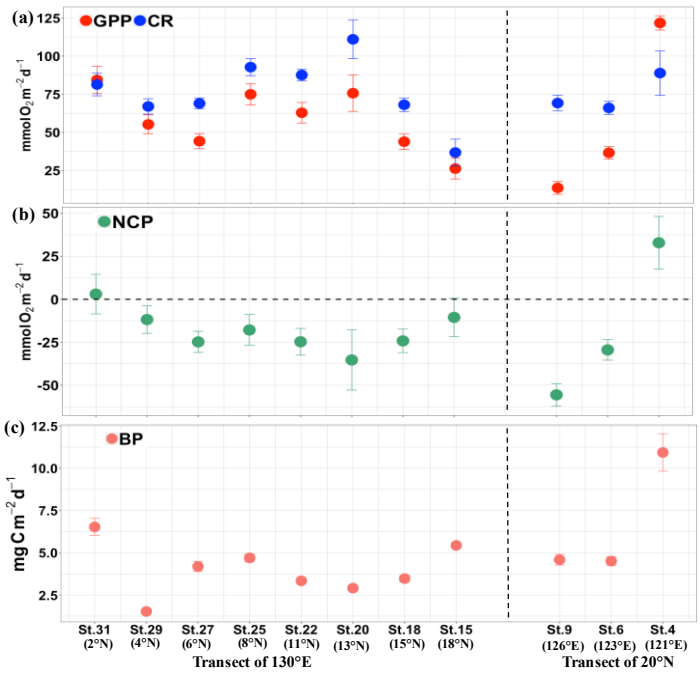

456

457 **Figure 5.** Spatial variations of integrated (a) gross primary production (GPP) and
458 community respiration (CR), (b) net community production (NCP), and (c) bacterial
459 production (BP) along the north-south transect at 130°E and the east-west transect at
460 20°N in the western Pacific Ocean. The error bars represent the standard errors of the
461 measurements.

462

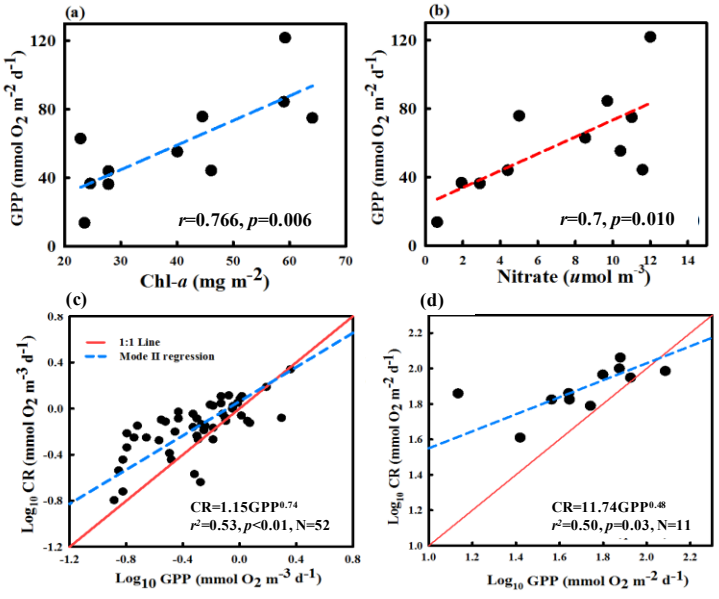

463

Figure 6. (a) Pearson correlation between integrated gross primary production (GPP) and integrated Chl-*a*. (b) Pearson correlation between integrated gross primary production (GPP) and average nitrate concentration in the upper 300 m. (c) Regression between volumetric GPP and community respiration (CR). (d) Regression between integrated GPP and CR in the western Pacific Ocean.

Table 2. Pearson correlations of the integrated metabolic rates with environmental variables (n = 11). The *p* values are shown in the brackets. The significant relationships are shown in bold ($p < 0.05$). ∫ GPP: gross primary production. ∫ CR: community respiration. ∫ NCP: net community production. ∫ BP: integrated bacterial production rate. SST: surface temperature. SS: surface salinity. ∫ Chl-*a*: integrated chlorophyll *a*.

	∫Chl-*a*	**Surface Chl-*a***	**SST**	**SS**	**Nitrate gradient**	**∫CR**	**∫NCP**	**∫BP**
∫ GPP	**0.73 (0.011)**	0.41 (0.212)	0.08 (0.819)	**-0.68 (0.020)**	**0.75 (0.002)**	**0.70 (0.015)**	**0.72 (0.013)**	0.63 (0.064)
∫ CR	0.47 (0.148)	0.41 (0.216)	0.23 (0.497)	-0.25 (0.461)	0.31 (0.351)		0.01 (0.968)	0.14 (0.679)
∫ NCP	0.57 (0.066)	0.14 (0.678)	-0.11 (0.750)	**-0.72 (0.012)**	**0.70 (0.013)**			0.41 (0.208)
∫ BP	0.30 (0.372)	-0.01 (0.995)	-0.43 (0.186)	-0.41 (0.215)	-0.11 (0.742)			

In general, the pooled dataset for these two transects suggests that the spatial variation of GPP was greater than that of CR, which is reflected by the larger coefficient of variation of the integrated GPP (52%) than that of CR (27%). The euphotic zone integrated GPP was positively correlated with the integrated Chl-*a* (r = 0.76, p = 0.011; Table 2, Fig. 6a) and the nitrate gradient across the base of the euphotic zone (r = 0.70, p = 0.001; Table 2, Fig. 6b). The CR can be regressed to GPP using the equations $CR = 1.15 * GPP^{0.74}$ (r^2 = 0.53, $p < 0.001$; Fig. 6c) for the volumetric values and $CR = 11.74 * GPP^{0.48}$ (r^2 = 0.50 p =0.03; Fig. 6d) for the integrated values. The slopes of the equations for GPP and CR indicate that the CR rates were slightly higher than the GPP; therefore, negative NCP prevailed at most of the stations. Based on the relationship between the GPP and CR, the thresholds of the euphotic zone integrated and volumetric GPP (below which the system is net heterotrophic) were 110 mmol O_2 m^{-2} d^{-1} and 1.7 mmol O_2 m^{-3} d^{-1}, respectively.

Bacterial production

Along the 130°E transect, the volumetric BP varied between 0.01 mg C m^{-3} d^{-1} and 0.076 mg C m^{-3} d^{-1} with a mean value of 0.056 mg C m^{-3} d^{-1} (Fig. 4d). We observed maxima of the volumetric BP in the intermediate layer along this transect (Fig. 4d). Along the 20°N transect, the volumetric BP at the eastern stations tended to be lower than those at the western stations (Fig. 4h). The maximum volumetric BP of 0.53 mg C m^{-3} d^{-1} was found at the surface at St. 4, which was consistent with the maximum volumetric GPP and CR (Fig. 4h). In terms of depth-integrated values, the

integrated BP did not show a pronounced spatial pattern in either the latitudinal or meridional transects (Fig. 5c). Except for the two peak values at St. 31 and St. 4, the integrated BPs along the two transects were both relatively constant and had intermediate values (Fig. 5c). The correlation between the integrated GPP and BP for the pooled dataset of the two transects was insignificant (Pearson $p = 0.06$).

Comparison of metabolism estimates derived from the *in vitro* incubations, geochemical model and empirical estimation

A comparison of the integrated metabolism derived from the *in vitro* incubations and the geochemical model along the two transects is presented in Fig. 7. In general, the model of *Letscher and Moore* [2017] predicted moderate autotrophy in this region during September and October, with an average NCP of 7 mmol O_2 m^{-2} d^{-1} (Fig. 7a). By contrast, our measurements indicated a prevalence of net heterotrophic conditions in this region (Fig. 7a). Similar to our field observations of higher metabolism rates at low latitudes, the GPPs predicted from the geochemical model had slightly higher values at the low latitude stations, although the spatial variability was less pronounced than our field observations (Fig. 7b) The GPPs estimated from the geochemical model along the two transects ranged from 42 mmol O_2 m^{-2} d^{-1} to 67 mmol O_2 m^{-2} d^{-1}, yielding no statistical differences with the GPPs measured by O_2-based incubation ($p = 0.90$ for the model output in September and $p = 0.86$ for the model output in October, paired *t*-test; Fig. 8b). However, our field-observed CRs were statistically higher than those predicted by the geochemical model during September (paired *t*-test, $p < 0.001$) and October (paired *t*-test, $p < 0.001$; Fig. 8c).

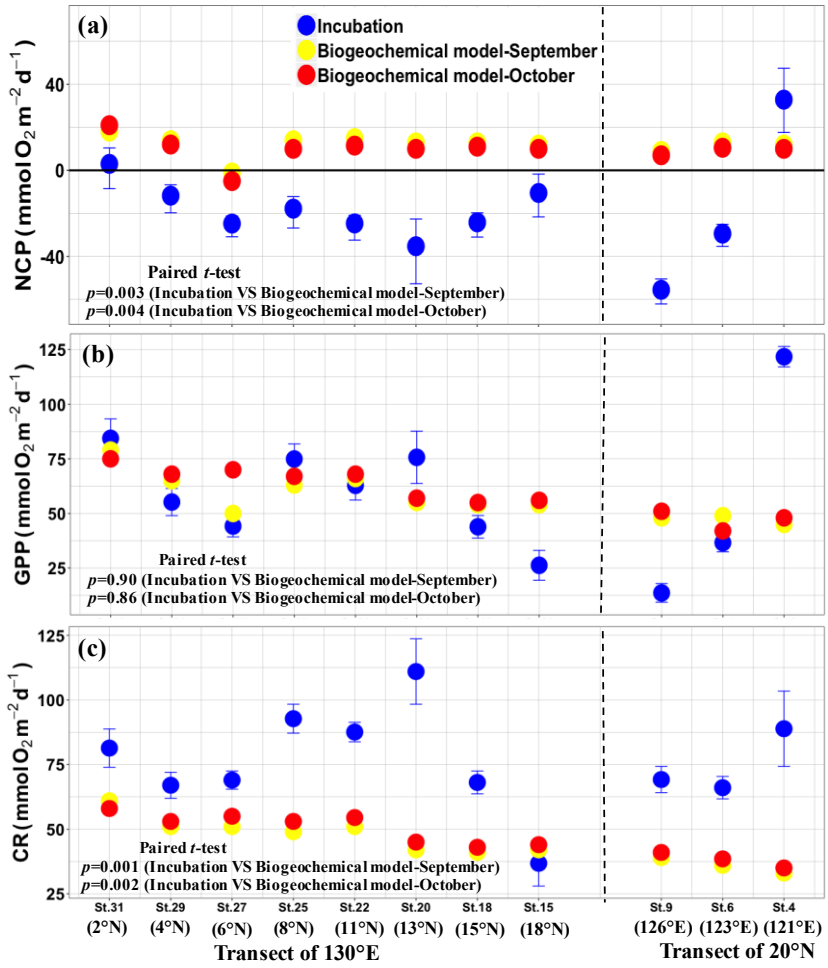

Figure 7. Comparison between the integrated metabolism at each sampling station derived from O_2-based incubation and the geochemical model of Letscher and Moore (2017). GPP: gross primary production; CR: community respiration; NCP: net community production.

The comparison of the CRs from the empirical estimates and the oxygen-based incubation approach showed that at 8 of the 11 stations, the measured CR exceeded the upper boundary of the empirical CR estimates, leaving a mean of 24 mmol O_2 m^{-2} d^{-1} of respiration unaccounted for in this region (Fig. 8). Conversely, most of the CRs predicted by the biogeochemical model of *Letscher and Moore* [2017] fell within the range of values derived from the empirical estimations (Fig. 8).

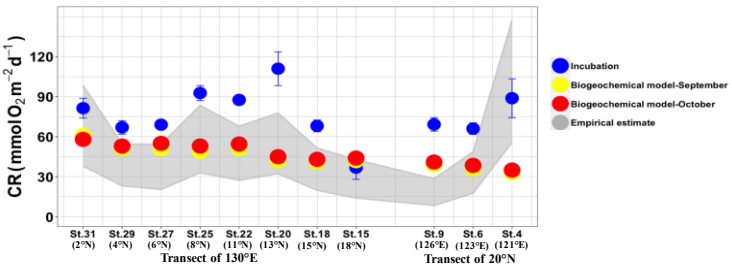

Figure 8. Comparison of the community respirations (CRs) derived from O_2-based incubation, empirical estimates and the geochemical model of *Letscher and Moore* [2017].

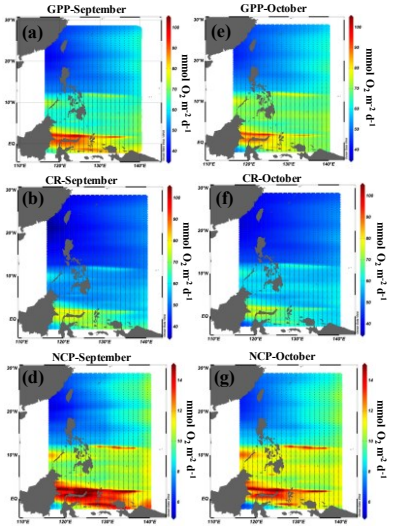

Figure S2. The integrated metabolism in the western Pacific Ocean within the euphotic zone during September and October derived from the biogeochemical model of Letscher and Moore (2017). GPP: gross primary production; CR: community respiration; NCP: net community production.

Discussion

The limited and uneven geographic distributions of the measured metabolic rates in the global ocean and reconciling the results of the metabolic balance derived from the incubation approach and the biochemical budget in a meaningful way remain major obstacles to a comprehensive understanding of the trophic status in the oligotrophic ocean [*Ducklow and Doney*, 2013; *Westberry et al.*, 2012]. This study contributes to the currently limited dataset in the western boundary currents of the

North Pacific Ocean and, and more broadly, adds insight into the unresolved debate about the autotrophy versus heterotrophy in the oligotrophic ocean.

Discrepancy of the regional metabolic state between the incubation and geochemical model predictions

The comparisons between the regional metabolic rates from the incubation approach and the model outputs address our first question. As we expected, the observations based on the oxygen changes during incubation exhibited a prevalence of net heterotrophic states in the warm and oligotrophic western Pacific Ocean. More than 80% of the volumetric NCP values were negative (Fig. 4c and 4g), and 8 of the 11 stations showed net heterotrophic states integrated over the entire water column (Fig. 5c). In this region, the environmental conditions feature high surface temperatures (>28 °C) and very low nutrient availability in the upper layers (Fig. 3). The mean Chl-*a* and volumetric GPP were only approximately 0.14 mg m^{-3} and 1.6 mmol O_2 m^{-3} d^{-1}, respectively, which fall into the conditions for a heterotrophic state according to the scaling laws proposed by *C. M. Duarte et al.* [2013].

However, the model of *Letscher and Moore* [2017] predicted a moderately autotrophic state in the western Pacific Ocean (Fig. 7a), which supports the metabolic state in the oligotrophic ocean that has been diagnosed by incubation-free methods in many previous studies [*Emerson*, 2014; *B Yang et al.*, 2017a]. Further comparisons of GPP and CR imply that our measured GPP values were consistent with the geochemistry-based values, but there was an apparent anomaly in the CR between

these two approaches (Fig. 7b and 7c). At the global scale, the validity of gross O_2 production rates has been tested in numerous studies by comparing concurrent measurements of primary production determined from ^{14}C incorporation [*Bender et al.*, 1999; *Grande et al.*, 1989; *Michael et al.*, 1987]. These results suggest that the GPP measured from *in vitro* O_2 change incubation generally tracks the distributions of ^{14}C-based primary production and could represent the true rates of autotrophic production. In this study, our measured GPPs were consistent with the changes in nutrient availability and Chl-*a* concentrations at regional scales (Fig. 6a and 6b). In the broader Pacific Ocean, our regional mean GPP values (59.8 ± 8.7 mmol O_2 m^{-2} d^{-1}) were similar to the primary production in the central gyre of the North Pacific, which has similarly oligotrophic conditions (61 ± 5.9 mmol O_2 m^{-2} d^{-1},*P J L B Williams et al.* [2004]), but were significantly lower than the corresponding rates previously reported in the eastern equatorial Pacific (211 ± 64 mmol O_2 m^{-2} d^{-1}; *Wambeke et al.* [2008]) and western subarctic Pacific (78 ± 24 mmol O_2 m^{-2} d^{-1}; *Furuya* [1995]), as determined by similar approaches. This latitudinal tendency of the GPP reflected by oxygen-based incubation is consistent with the current knowledge of higher nutrient availability in the colder and well-mixed Arctic water and the widespread occurrence of upwelling systems in the equatorial ocean, which adds further evidence of the rationality of GPP measurements at both regional and latitudinal scales.

In contrast to the consistency of the GPP between the incubation and biogeochemical model outputs, most of the CRs derived from the incubation approach

exceeded the model predictions (Fig. 7c). In addition to the locally produced organic carbon, the model simulation of *Letscher and Moore* [2017] explicitly included the fluxes of semi-labile organic carbon and the lateral supply of allochthonous and terrigenous organic carbon, which are considered a key pathway to fuel the respiration if the prevalent heterotrophy is real. The apparent CR anomaly implies that *in vitro* estimates of CR are difficult to reconcile from the perspective of biogeochemical cycles. Unlike primary production, for which several independent incubation approaches (i.e., ^{14}C-based incorporation rates) can be used to constrain the global magnitude and trends, it appears that there is no comparable incubation approach to directly measure the CR except for the oxygen consumption in dark bottles. Similar to many previous studies that showed the relative constancy of the geographical patterns of CR [*Aranguren-Gassis et al.*, 2011; *Morán et al.*, 2004; *Wang et al.*, 2014], our depth-integrated CRs tended to be less variable than the GPPs, which casts further doubt on the accuracy of CR measurements.

Reconciling the signal of community respiration determined by the incubation

The comparison between the incubation results and model outputs appears to support our GPP measurements, but it leaves some doubts about the magnitude of the *in vitro* CR. To further validate the CR between the model output and incubation approach, we performed another independent estimate of the respiration contributed by the major trophic groups of plankton at each station (Table 1) with the goal of constraining the possible CR based on the magnitude of the measured GPP and BP.

Heterotrophic bacteria have long been considered to perform most of the respiration in the open ocean; therefore, individual measurements of BP are also a key factor influencing the magnitudes of our empirical CR estimates. The average rates of BP in our study region were at the low end of previously reported values in the Pacific systems and other oligotrophic systems (Table 3). The calculated BP requires a conversion factor to transform the leucine incorporation rates into carbon production. Low leucine incorporation rates are typically found in oligotrophic, subtropical waters, and our measured leucine incorporation rates were comparable with the values in the oligotrophic ocean in ALOHA [*Viviani and Church*, 2017]. Therefore, the major possible cause of low BP might be related to the conversion factor of leucine to carbon. In many previous studies, an empirical value of the leucine-to-carbon conversion factor (i.e., 1.5 kg C mol leu^{-1}) was used assuming no isotopic dilution [*Kirchman*, 1993]. Growing experimental evidence suggests that CF depends in part on the composition of the substrates and the nutrient status and that it decreases markedly from the coastal areas to the open ocean [*Alonso-Sáez et al.*, 2007; *Zubkov et al.*, 2000b]. Our measured CF values (average of 0.37 kg C mol Leu^{-1}) are well within the range of measured CFs in the oligotrophic system [*Alonso-Sáez et al.*, 2007; *Vázquez-Domínguez et al.*, 2008; *Zubkov et al.*, 2000b], which further indicates that the application of theoretical values of CF may potentially overestimate the bacterial activity in the oligotrophic ocean.

Table 3. Review of euphotic zone integrated bacterial metabolism (mean ± standard error) in the Pacific Ocean, adjacent ocean and subtropical oceans.

Region	Leu incorporation	Leu CF	Bacterial Production	References
	pmol m^{-2} h^{-1}	Kg C mol^{-1} leu	mg C m^{-2} d^{-1}	
Northern Pacific gyre	739 ± 140	1.5	27 ± 2.1	*Viviani and Church* [2017]
Eastern South Pacific	4360 ± 1200	1.5	160 ± 46	*Wambeke et al.* [2008]
Western subarctic Pacific	1572 ± 740	1.06	40 ± 14	*Sherry et al.* [2002]
Northern South China Sea	3941 ± 1200	0.37	35 ± 7.2	*Wang et al.* [2014]
Northern Atlantic gyre	958 ± 123	0.73	17 ± 2.3	Morán et al. (2007)
Western Pacific boundary	627 ± 260	0.37	5.6 ± 1.2	This study

We found that an appreciable amount of measured CR could not be completely explained by the sum of the independent assessments of the different trophic groups at most of the stations (Fig. 8). Although considerable errors are associated with the CR estimates for each group, the results showed that even under the conditions of the maximum possible contribution, it is still difficult to bridge the gap between the *in vitro* measured respiration and the estimated respiration. Interestingly, most of the CRs predicted by the geochemical model fell within the possible range of the empirically estimated CRs, which in turn provides cross-validation of the rationality

of the CR predicted by the geochemical model (Fig. 8). This analysis thus reveals that *in vitro* measurements of CR, rather than GPP measurements, are most likely responsible for the observation of net heterotrophy in this area. A similar finding was reported by *Morán et al.* [2007], who demonstrated that in the North Atlantic gyre, approximately 48% of the measured CR from changes in oxygen in dark bottles could not be explained by the contributions of trophic groups of plankton. The author related this discrepancy to the fundamental flaw associated with long-term dark incubation (24 h) in an enclosed system. Several previous studies highlighted the diel synchrony of the growth of photosynthetic prokaryotes in cultures and the ocean [*Jacquet et al.*, 2001; *Zubkov et al.*, 2000a]. Long-term dark incubation might disrupt the diel synchrony of the dominant community of picoplankton. In spite of the still unclear consequences of this effect, it is likely that rapid disruption of the diel synchrony would lead to an elevation of the metabolic cost (i.e., respiration) for picoplankton under stress. Increases in bacterial abundances and substrate assimilation rates during bottle incubation have been revealed due to the exclusion of large zooplankton that feed on microheterotrophs, especially in oligotrophic systems characterized by tightly coupled microbial communities [*Evelyn et al.*, 1999; *Pomeroy et al.*, 1994]. This effect of eliminating large predators in respiration measurements would be more apparent in the size-fraction incubation when >1 μm organisms were removed, yielding a 50% overestimation of respiration in the bottle [*Aranguren-Gassis et al.*, 2012]. In addition, "new surfaces" for bacterial attachment in the container may be favorable for the growth of attached bacteria, enhancing respiration

during bottle incubation. However, the precise mechanism of the overestimation of CR by *in vitro* incubations is beyond the scope of our current data. A useful caveat of our study might be a request to further check the possible methodological problem, especially that associated with dark incubation.

Conclusion

This study is the first to report plankton community and bacterial metabolism on the western boundary of the northern Pacific Ocean based on *in vitro* incubation. The combination of analyses across different approaches allows us to enhance our understanding of the metabolic state of the oligotrophic ocean, particularly in the interpretation of net heterotrophy determined from light-dark bottles. Our comparison with the biogeochemical model and the contributions of major plankton groups suggests that the negative NCP may stem from systematically overestimated *in vitro* measured CR, although the exact cause of the problem is unresolved and requires further study.

References

Alonso-Sáez, L., J. M. Gasol, J. Arístegui, J. C. Vilas, D. Vaqué, C. M. Duarte, and S. Agustí (2007), Large-scale variability in surface bacterial carbon demand and growth efficiency in the subtropical northeast Atlantic Ocean, *Limnology and Oceanography*, *52*(2), 533-546, doi:10.4319/lo.2007.52.2.0533.

Aranguren-Gassis, M., P. Serret, E. Fernandez, J. L. Herrera, J. F. Domínguez, V. Perez, and J. Escanez (2011), Production and respiration control the marine

microbial metabolic balance in the eastern North Atlantic subtropical gyre, *Deep Sea Research Part I: Oceanographic Research Papers*, *58*(7), 768-775, doi:10.1016/j.dsr.2011.05.003.

Aranguren-Gassis, M., E. Teira, M. Serret, S. Martínez-García, and E. Fernández (2012), *Potential overstimation of bacterial respiration rates in oligotrophic plankton communities*, 1 pp., Marine Ecology Progress, doi:10.3354/meps09707.

Arrigo, K. R. (2005), Erratum: Marine microorganisms and global nutrient cycles, *Nature*, *437*(7057), 349, doi:10.1038/nature04158.

Azam, F., T. Fenchel, J. G. Field, J. S. Gray, L. A. Meyerreil, and F. Thingstad (1983), The ecological role of water-column microbes in the sea, *Marine Ecology Progress Series*, *10*(3), 257-263, doi:10.3354/meps010257.

Bender, M., J. Orchardo, M.-L. Dickson, R. Barber, and S. Lindley (1999), In vitro O2 fluxes compared with 14C production and other rate terms during the JGOFS Equatorial Pacific experiment, *Deep Sea Research Part I: Oceanographic Research Papers*, *46*(4), 637-654, doi:10.1016/S0967-0637(98)00080-6.

Bjørnsen, P. K., and J. Kuparinen (1991), Determination of bacterioplankton biomass, net production and growth efficiency in the Southern Ocean, *Marine Ecology Progress*, *71*(2), 185-194.

Calbet, A., and M. R. Landry (2004), Phytoplankton growth, microzooplankton grazing, and carbon cycling in marine systems, *Limnology and Oceanography*,

49(1), 51-57, doi:10.4319/lo.2004.49.1.0051.

Carvalho, M. C., K. G. Schulz, and B. D. Eyre (2017), Respiration of new and old carbon in the surface ocean: implications for estimates of global oceanic gross primary productivity, *Global Biogeochemical Cycles*, *31*, 975–984, doi:10.1002/2016GB005583.

Chen, B., B. Huang, Y. Xie, C. Guo, S. Song, L. I. Hongbo, and H. Liu (2014), The bacterial abundance and production in the East China Sea: seasonal variations and relationships with the phytoplankton biomass and production, *Acta Oceanologica Sinica*, *33*(9), 166-177, doi: 10.1007/s13131-014-0528-0.

Clarke, G. L., and R. H. Oster (1934), The penetration of the blue and red componets of daylight into Atlantic coastal water and its realtion to phytoplankton metabolism *The Biological Bulletin*, *67*(1), 59-75, doi:10.2307/1537482.

Core, T. R. (2014), A language and environment for statistical computing, R foundation for statistical computing, Vienna, Austria., edited.

Del Giorgio, P. A., J. J. Cole, and A. Cimbleris (1997), Respiration rates in bacteria exceed phytoplankton production in unproductive aquatic systems, *Nature*, *385*(6612), 148-151, doi:10.1038/385148a0.

Duarte, C. M., and J. Cebrián (1996), The fate of marine autotrophic production, *Limnology and Oceanography*, *41*(8), 1758-1766, doi:10.4319/lo.1996.41.8.1758.

Duarte, C. M., A. Regaudie-de-Gioux, J. M. Arrieta, A. Delgado-Huertas, and

S. Agusti (2013), The oligotrophic ocean is heterotrophic, *Annual Review of Marine Science, Vol 5*, *5*(4), 551-569, doi:10.1146/annurev-marine-121211-172337.

Ducklow, H. W., and S. C. Doney (2013), What is the metabolic state of the oligotrophic ocean? A debate, *Annual Review of Marine Science*, *5*(1), 525-533, doi:10.1146/annurev-marine-121211-172331.

Emerson, S. (2014), Annual net community production and the biological carbon flux in the ocean, *Global Biogeochemical Cycles*, *28*(1), 14-28, doi:10.1002/2013gb004680.

Evelyn, B. S., F. S. Barry, and T. S. Crystal (1999), Activity of marine bacteria under incubated and in situ conditions, *Aquatic Microbial Ecology*, *20*(3), 213-223, doi:10.3354/ame020213.

Field, C. B., M. J. Behrenfeld, J. T. Randerson, and P. Falkowski (1998), Primary production of the biosphere: integrating terrestrial and oceanic components, *Science*, *281*(5374), 237-240, doi:10.1126/science.281.5374.237.

Fine, R. A., R. Lukas, F. M. Bingham, M. J. Warner, and R. H. Gammon (1994), The western equatorial Pacific: A water mass crossroads, *Journal of Geophysical Research: Oceans*, *99*(C12), 25063-25080, doi:10.1029/94JC02277.

Fukuda, R., H. Ogawa, T. Nagata, and I. Koike (1998), Direct determination of carbon and nitrogen contents of natural bacterial assemblages in marine environments, *Applied and Environmental Microbiology*, *64*(9), 3352-3358.

Furuya, O. a. (1995), Primary production and community respiration in the subarctic water of the western North Pacific, *Biogeochemical Processes and Ocean Flux in the Western Pacific, Terra Scientific Publishing, Tokyo (1995), pp. 239-253*.

Giorgio, P. A. D., P. J. B. Williams, P. A. D. Giorgio, and P. J. B. Williams (2005), Respiration in aquatic ecosystems, *Oxford Oxford University Press 25*(1), 100.

Grande, K. D., P. J. L. Williams, J. Marra, D. A. Purdie, K. Heinemann, R. W. Eppley, and M. L. Bender (1989), Primary production in the North Pacific gyre: a comparison of rates determined by the 14 C, O2 concentration and 18O methods, *Deep Sea Research Part A Oceanographic Research Papers*, *36*(11), 1621-1634, doi:10.1016/0198-0149(89)90063-0.

Hedges, J. I., J. A. Baldock, Y. Gélinas, C. Lee, M. L. Peterson, and S. G. Wakeham (2002), The biochemical and elemental compositions of marine plankton: A NMR perspective, *Marine Chemistry*, *78*(1), 47-63, doi:10.1016/S0304-4203(02)00009-9.

Hu, D., et al. (2015), Pacific western boundary currents and their roles in climate, *Nature*, *522*(7556), 299-308, doi:10.1038/nature14504.

Huang, Y., X. Liu, E. A. Laws, C. Bingzhang, Y. Li, Y. Xie, Y. Wu, K. Gao, and B. Huang (2018), Effects of increasing atmospheric CO2 on the marine phytoplankton and bacterial metabolism during a bloom: A coastal mesocosm study, *Science of the Total Environment*, *633*, 618-629, doi:10.1016/j.scitotenv.2018.03.222.

Jacquet, S., F. Partensky, J. F. Lennon, and D. Vaulot (2001), Diel patterns of growth and division in marine picoplankton in culture, *Journal of Phycology*, *37*(3), 357–369, doi:10.1046/j.1529-8817.2001.037003357.x.

Jiao, N., et al. (2010), Microbial production of recalcitrant dissolved organic matter: long-term carbon storage in the global ocean, *Nature Reviews Microbiology*, *8*, 593, doi:10.1038/nrmicro2386.

Kirchman, D. (1993), Leucine incorporation as a measure of biomass production by heterotrophic bacteria, *Handbook of Methods in Aquatic Microbial Ecology. Lewis*, 509-512.

Kyewalyanga, M., T. Platt, and S. Sathyendranath (1992), Ocean primary production calculated by spectral and broad-band models, *Marine Ecology Progress Series*, *85*(1/2), 171-185.

Laws, E. A. (1991), Photosynthetic quotients, new production and net community production in the open ocean, *Deep Sea Research Part I 38*(1), 143-167, doi:10.1016/0198-0149(91)90059-O.

Laws, E. A., G. R. DiTullio, K. L. Carder, P. R. Betzer, and S. Hawes (1990), Primary production in the deep blue sea, *Deep Sea Research Part A. Oceanographic Research Papers*, *37*(5), 715-730, doi:https://doi.org/10.1016/0198-0149(90)90001-C.

Letscher, R. T., and J. K. Moore (2017), Modest net autotrophy in the oligotrophic ocean, *Global Biogeochemical Cycles*, *31*, 699–708, doi:10.1002/2016GB005503.

Longhurst, A. (1995), Seasonal cycles of pelagic production and consumption, *Progress in Oceanography*, *36*(2), 77-167, doi:10.1016/0079-6611(95)00015-1.

López-Urrutia, Á., and X. A. G. Morán (2007), Resource limitation of bacterial production distorts the temperature dependence of oceanic carbon cycling, *Ecology*, *88*(4), 817-822, doi:10.1890/06-1641.

López-Urrutia, Á., E. San Martin, R. P. Harris, and X. Irigoien (2006), Scaling the metabolic balance of the oceans, *Proceedings of the National Academy of Sciences*, *103*(23), 8739.

Marra, J., and R. T. Barber (2004), Phytoplankton and heterotrophic respiration in the surface layer of the ocean, *Geophysical Research Letters*, *31*(9), L09314, doi:10.1029/2004GL019664.

Michael, B., G. Karen, J. Kenneth, M. John, W. P. J. LeB, S. John, P. Michael, L. Chris, H. Gary, and O. Joseph (1987), A comparison of four methods for determining planktonic community production, *Limnology and Oceanography*, *32*(5), 1085-1098, doi:10.4319/lo.1987.32.5.1085.

Miller, J. C., and J. N. Miller (1988), Statistics for analytical chemistry, 2nd edition, *Analytical and Bioanalytical Chemistry*, *378*(7), 1676-1677.

Morán, X. A. G., E. Fernández, and V. Pérez (2004), Size-fractionated primary production, bacterial production and net community production in subtropical and tropical domains of the oligotrophic NE Atlantic in autumn, *Marine Ecology Progress Series*, *274*, 17-29, doi:10.3354/meps274017.

Morán, X. A. G., V. Pérez, and E. Fernández (2007), Mismatch between community respiration and the contribution of heterotrophic bacteria in the NE Atlantic open ocean: What causes high respiration in oligotrophic waters?, *Journal of Marine Research*, *65*(4), 545-560, doi:10.1357/002224007782689102.

Oudot, C., R. Gerard, P. Morin, and I. Gningue (1988), Precise shipboard determination of dissolved-oxygen (Winkler procedure) for productivity studies with a commercial system, *Limnology and Oceanography*, *33*(1), 146-150, doi:10.4319/lo.1988.33.1.0146.

Pomeroy, L. R., J. E. Sheldon, and W. M. S. Jr (1994), Changes in bacterial numbers and leucine assimilation during estimations of microbial respiratory rates in seawater by the precision Winkler method, *Applied and Environmental Microbiology*, *60*(1), 328-332.

Regaudie-de-Gioux, A., and C. M. Duarte (2012), Temperature dependence of planktonic metabolism in the ocean, *Global Biogeochemical Cycles*, *26*(1), GB1015, doi:10.1029/2010GB003907.

Rivkin, R. B., and L. Legendre (2001), Biogenic carbon cycling in the upper ocean: effects of microbial respiration, *Science*, *291*(5512), 2398-2400, doi:10.1126/science.291.5512.2398.

Robinson, C., P. Serret, G. Tilstone, E. Teira, M. V. Zubkov, A. P. Rees, and E. M. S. Woodward (2002), Plankton respiration in the Eastern Atlantic Ocean, *Deep Sea Research Part I: Oceanographic Research Papers*, *49*(5), 787-813,

doi:10.1016/S0967-0637(01)00083-8.

Robinson, C., and P. J. L. B. Williams (2005), *Chapter 9. Respiration and its measurement in surface marine waters*, 147-181 pp.

Roland, F., and J. J. Cole (1999), Regulation of bacterial growth efficiency in a large turbid estuary, *Aquatic Microbial Ecology*, *20*(1), 31-38, doi:10.3354/ame020031.

Schlitzer, R. (2012), Ocean data view Available at odv.awi.de. Accessed November 3, 2013, edited.

Serret, P., E. Fernandez, J. A. Sostres, and R. Anadon (1999), Seasonal compensation of microbial production and respiration in a temperate sea, *Marine Ecology Progress Series*, *187*, 43-57, doi:10.3354/meps187043.

Serret, P., C. Robinson, M. Aranguren-Gassis, E. E. Garcia-Martin, N. Gist, V. Kitidis, J. Lozano, J. Stephens, C. Harris, and R. Thomas (2015), Both respiration and photosynthesis determine the scaling of plankton metabolism in the oligotrophic ocean, *Nature Communications*, *6*, 6961, doi:1038/ncomms7961.

Sherry, N. D., B. Imanian, K. Sugimoto, P. W. Boyd, and P. J. Harrison (2002), Seasonal and interannual trends in heterotrophic bacterial processes between 1995 and 1999 in the subarctic NE Pacific, *Deep Sea Research Part II: Topical Studies in Oceanography*, *49*(24), 5775-5791, doi:10.1016/S0967-0645(02)00214-X.

Shiozaki, T., K. Furuya, T. Kodama, and S. Takeda (2009), Contribution of N2

fixation to new production in the western North Pacific Ocean along 155°E, *Marine Ecology Progress*, *377*(1), 19-32, doi:10.3354/meps07837.

Sigman, D. M., and E. A. Boyle (2000), Glacial/interglacial variations in atmospheric carbon dioxide, *Nature*, *407*(6806), 859-869, doi:10.1038/35038000.

Vázquez-Domínguez, E., C. M. Duarte, S. Agustí, K. Jürgens, D. Vaqué, and J. M. Gasol (2008), Microbial plankton abundance and heterotrophic activity across the Central Atlantic Ocean, *Progress in Oceanography*, *79*(1), 83-94, doi:10.1016/j.pocean.2008.08.002.

Verity, P. G. (1985), Grazing, respiration, excretion, and growth rates of tintinnids1, *Limnology and Oceanography*, *30*(6), 1268-1282, doi:10.4319/lo.1985.30.6.1268.

Viviani, D. A., and M. J. Church (2017), Decoupling between bacterial production and primary production over multiple time scales in the North Pacific Subtropical Gyre, *Deep Sea Research Part I: Oceanographic Research Papers*, *121*(1), 132-142, doi:10.1016/j.dsr.2017.01.006.

Wambeke, F. V., I. Obernosterer, T. Moutin, S. Duhamel, O. Ulloa, and H. Claustre (2008), Heterotrophic bacterial production in the eastern South Pacific: longitudinal trends and coupling with primary production, *Biogeosciences*, *5*(1), 157-169, doi:10.5194/bg-5-157-2008.

Wang, N., W. Lin, B. Chen, and B. Huang (2014), Metabolic states of the Taiwan Strait and the northern South China Sea in summer 2012 (In Chinese

with English abstract), *Journal of Tropical Oceanography*, *33*(4), 61-68.

Welschmeyer, N. A. (1994), Fluorometric analysis of chlorophyll a in the presence of chlorophyll b and pheopigments, *Limnology and Oceanography*, *39*(8), 1985-1992, doi:10.4319/lo.1994.39.8.1985.

Westberry, T. K., P. J. l. B. Williams, and M. J. Behrenfeld (2012), Global net community production and the putative net heterotrophy of the oligotrophic oceans, *Global Biogeochemical Cycles*, *26*(4), n/a-n/a, doi:10.1029/2011GB004094.

Williams, P. J. L., P. D. Quay, T. K. Westberry, and M. J. Behrenfeld (2013), The oligotrophic ocean is autotrophic, *Annual Review of Marine Science, Vol 5*, *5*(1), 535-549, doi:10.1146/annurev-marine-121211-172335.

Williams, P. J. L. B., P. J. Morris, and D. M. Karl (2004), Net community production and metabolic balance at the oligotrophic ocean site, station ALOHA, *Deep Sea Research Part I Oceanographic Research Papers*, *51*(11), 1563-1578, doi:10.1016/j.dsr.2004.07.001.

Yang, B., S. R. Emerson, and S. M. Bushinsky (2017a), Annual net community production in the subtropical Pacific Ocean from in-situ oxygen measurements on profiling floats, *Global Biogeochemical Cycles*, *31*, 728–744, doi:10.1002/2016GB005545.

Yang, G., C. Li, K. Guilini, X. Wang, and Y. Wang (2017b), Regional patterns of δ 13 C and δ 15 N stable isotopes of size-fractionated zooplankton in the western tropical North Pacific Ocean, *Deep-Sea Res. Part I Oceanogr. Res.*

Pap., *120*, 39-47, doi:10.1016/j.dsr.2016.12.007.

Yang, G., C. Li, Y. Wang, X. Wang, L. Dai, Z. Tao, and P. Ji (2017c), Spatial variation of the zooplankton community in the western tropical Pacific Ocean during the summer of 2014, *Continental Shelf Research*, *135*, 14-22, doi:10.1016/j.csr.2017.01.009.

Zubkov, M. V., M. A. Sleigh, and P. H. Burkill (2000a), Assaying picoplankton distribution by flow cytometry of underway samples collected along a meridional transect across the Atlantic Ocean, *Aquatic Microbial Ecology*, *21*(1), 13-20, doi:10.3354/ame021013.

Zubkov, M. V., M. A. Sleigh, P. H. Burkill, and R. J. G. Leakey (2000b), Bacterial growth and grazing loss in contrasting areas of North and South Atlantic, *Journal of Plankton Research*, *22*(4), 685-711, doi:10.1093/plankt/22.4.685.